Advances and Applications in Fluid Mechanics
© 2013 Pushpa Publishing House, Allahabad, India
Published Online: January 2014
Available online at http://pphmj.com/journals/aafm.htm
Volume 14, Number 2, 2013, Pages 169-200

RADIATION EFFECT ON AN MHD FREE CONVECTIVE FLOW THROUGH A CHANNEL BOUNDED BY A LONG WAVY WALL AND A PARALLEL FLAT WALL WITH SORET AND DUFOUR EFFECTS

N. Ahmed and D. J. Bhattacharyya

Department of Mathematics
Gauhati University
Guwahati 781 014, Assam, India
e-mail: saheel_nazib@yahoo.com
shandilyadhruva@gmail.com

Abstract

A parametric study to investigate the effect of radiation on a two dimensional free convective MHD flow of a viscous incompressible and electrically conducting fluid through a channel bounded by a long vertical wavy wall and a parallel flat wall with Soret and Dufour effects is presented. A uniform magnetic field is assumed to be applied normal to the flat wall. The equation governing fluid flow is solved analytically subject to the relevant boundary conditions. It is assumed that the solution consists of two parts, a mean part and a perturbed part. The long wave approximation has been used to obtain the solution of the perturbed part and to solve the mean part, the well known approximation used by Ostrach [1] has been applied. The perturbed part of the solution is the contribution from the waviness of the wall. The expressions for zeroth and first order velocity, temperature, concentration and skin friction and the rates of heat and

Received: May 14, 2013; Accepted: September 13, 2013
2010 Mathematics Subject Classification: 76W05.
Keywords and phrases: MHD, free convective, radiation effect, Soret effect, Dufour effect.
Communicated by Shahrdad G. Sajjadi

mass transfer at the walls are obtained. Some of the results indicating the influence of radiation, Soret and Dufour effects on the above fields have been presented graphically.

Nomenclature

K_λ	Absorption coefficient
g	Acceleration due to gravity
ε	Amplitude parameter
$\bar{x}$, $\bar{y}$	Cartesian coordinates
μ	Coefficient of viscosity
β	Coefficient of volume expansion for heat transfer
C_s	Concentration susceptibility
D_M	Coefficient of mass diffusion
Q	Constant heat addition/absorption
d	Distance between two walls
ρ_s	Density of the fluid in static condition
D_u	Dufour number
σ	Electrical conductivity
$\bar{p}$	Fluid pressure
ρ	Fluid density
λ	Frequency parameter
$\bar{T}$	Fluid temperature
$\bar{T}_s$	Fluid temperature in static condition
G_r	Grashof number for heat transfer
G_m	Grashof number for mass transfer

α	Heat source parameter
υ	Kinematic viscosity
T_m	Mean fluid temperature
M	Magnetic parameter
$e_{b\lambda}$	Plank function
$\bar{p}_s$	Pressure of the fluid in static condition
P_r	Prandtl number
N	Radiation parameter
$\bar{B}$	Strength of the applied magnetic field
$\bar{C}$	Species concentration
C_p	Specific heat at constant pressure
$\bar{C}_w$	Species concentration at the wavy wall
$\bar{C}_1$	Species concentration at the flat wall
S_r	Soret number
S_c	Schmidt number
k	Thermal conductivity
$\bar{T}_w$	Temperature of the wavy wall
$\bar{T}_1$	Temperature of the flat wall
K_T	Thermal-diffusion ratio
$\bar{u}$, $\bar{v}$	Velocity components
$\bar{\beta}$	Volumetric coefficient of the expansion with species concentration
m	Wall temperature ratio
n	Wall concentration ratio

Introduction

The incompressible boundary layer flow over a wavy wall has got importance because of its application in different areas such as cross-hatching on ablative surface, transpiration cooling of re-entry vehicle and rocket booster and film vaporization in combustion chambers. Lekoudis et al. [2] made a linear analysis of compressible boundary layer flows over a wavy wall. The Rayleigh problem for wavy wall had been studied by Shankar and Sinha [3]. They arrived at a certain interesting conclusion that at low Reynolds numbers, the waviness of the wall quickly ceases to be importance as the liquid is dragged along by the wall, while at large Reynolds numbers, the effect of viscosity is confined to a thin layer closed to the wall and known potential solution emerges in time. The analysis of the effect of small amplitude wall waviness upon the stability of the laminar boundary layer was made by Lessen and Gangwani [4]. Vajravelu and Sastri [5] made an analysis of the free convective heat transfer in a viscous incompressible fluid between a long vertical wavy wall and a parallel flat wall. Further they extended their work for vertical wavy channels. Rao and Sastri [6] studied the work of Vajravelu and Sastri [7] for viscous heating effects when the fluid properties are constants and variables. Again Rao [8] reinvestigated the problem of Rao and Sastri [6] for the channels which are of different wave numbers. Das and Ahmed [9] studied the free convection MHD flow and heat transfer in a viscous incompressible fluid confined between a long vertical wavy wall and a parallel flat wall. In the above mentioned works, the diffusion-thermo (Dufour) and the thermal-diffusion (Soret) terms were not taken into account in the energy and concentration equations, respectively. But when the heat and mass transfer occurs simultaneously in a moving fluid, the relations between the fluxes and driving potentials are of a more intricate nature. It is found that a heat flux can be generated not only by temperature gradients but by composition gradients as well. The heat flux that occurs due to composition gradient is called the *Dufour effect* or *diffusion-thermo effect*. On the other hand, the flux of mass caused due to temperature gradient is known as the Soret effect or the thermal-diffusion effect. The experimental investigation of the thermal-diffusion effect on mass transfer related problems was first done by Charles Soret in 1879. Hence this thermal-diffusion is known as the Soret effect in honour of Charles Soret. In general, the Soret and Dufour effects are of a smaller order of magnitude than the effects described in Fourier's or Fick's law and are often neglected in heat and mass transfer processes. Though these effects are quite small, but the devices can be arranged to produce very steep temperature and concentration gradients so that the separation of components in mixtures is affected. Eckert and Drake [10] have emphasized that the Soret effect assumes significance in cases concerning isotope separation and in mixtures between gases with very light molecular weight $(\mathrm{H}_2, \mathrm{He})$ and for medium molecular weight $(\mathrm{N}_2, \mathrm{air})$, the Dufour effect is found to be of considerable magnitude such that it cannot be ignored. Following Eckert and Drake's work [10], several other investigators have carried out model studies on the Soret and Dufour effects in different heat and mass transfer problems. Some of them are Dursunkaya and Worek [11], Kafoussias and Williams [12], Sattar and Alam [13], Alam et al. [14] and Raju et al. [15]. Recently, Ahmed et al. [16] have investigated the Soret and Dufour effects in free convection MHD flow of a viscous incompressible fluid through a channel bounded by a long vertical wavy wall and parallel flat wall.

Radiation is a process of heat transfer through electromagnetic waves. Radiative convective flows are encountered in countless industrial and environment processes, e.g., heating and cooling chambers, fossil fuel combustion energy processes, evaporation from large open water reservoirs, astrophysical flows, and solar power technology and space vehicle re-entry. Radiative heat and mass transfer plays an important role in manufacturing industries for the design of reliable equipment. Nuclear power plants, gas turbines and various propulsion devices for aircraft, missiles, satellites and space vehicles are examples of such engineering applications. If the temperature of the surrounding fluid is rather high, then radiation effects play an important role in space related technology. The effect of radiation on various convective flows under different conditions has been studied by many researchers including Hossain and Takhar [17], Ahmed and Sarmah [18], Rajesh and Varma [19] and Kesavaiah et al. [20]. As the present authors are ware, no attempt has been made till now, to study the effect of thermal radiation on an MHD free convective mass transfer flow through a channel bounded by a long wavy wall and a parallel flat wall with Soret and Dufour effects. Such an attempt has been made in the present paper owing to application of such types of problems in different engineering fields. This work is a generalization of the work studied by Ahmed et al. [16] to consider the radiation effect in addition to Soret and Dufour effects.

Basic Equations

We consider the two dimensional steady laminar free convective MHD flow along the vertical channel. The *x*-axis is taken parallel to the flat wall and *y*-axis is perpendicular to it. The wavy and the flat walls are represented by $\bar{y} = \bar{\varepsilon}\cos k\bar{x}$ and $\bar{y} = d$, respectively, $\bar{T}_w$ and $\bar{T}_1$ being their constant temperatures.

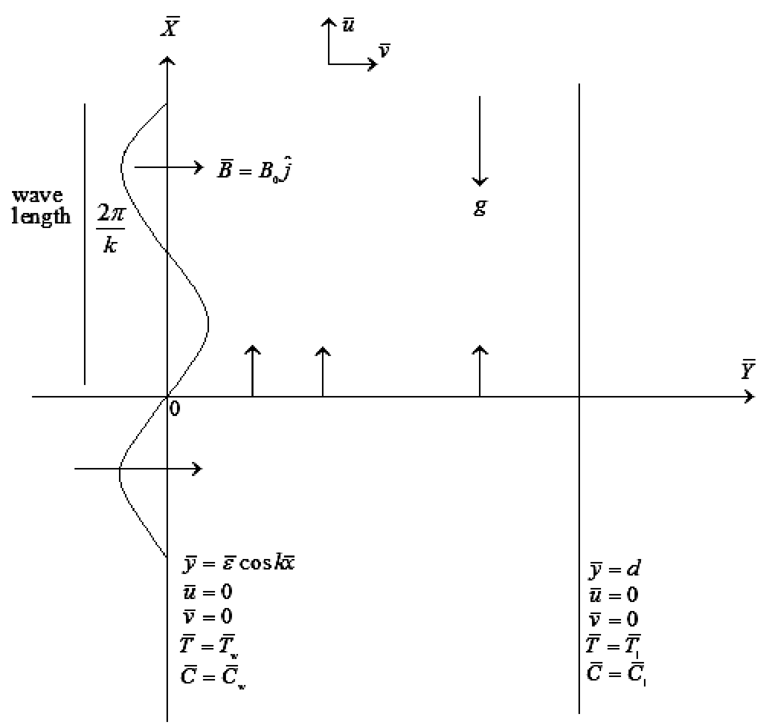

Flow configuration

Our investigation is restricted to the following assumptions:

(i) All the fluid properties except the density in the buoyancy force are constants.

(ii) The viscous and magnetic dissipation of energy are negligible.

(iii) The volumetric heat source/sink term in the energy equation is a constant.

(iv) The magnetic Reynolds number is small enough to neglect the induced magnetic field.

(v) The wavelength of the wavy wall, which is proportional to $1/k$, is large.

Under the foregoing assumptions, the equations which govern the two dimensional steady laminar free convective MHD flow and heat transfer in a viscous incompressible fluid occupying the channel are:

The momentum equations:

$$\rho\left[\bar{u}\frac{\partial\bar{u}}{\partial\bar{x}} + \bar{v}\frac{\partial\bar{u}}{\partial\bar{y}}\right] = -\frac{\partial\bar{p}}{\partial\bar{x}} + \mu\left[\frac{\partial^2\bar{u}}{\partial\bar{x}^2} + \frac{\partial^2\bar{u}}{\partial\bar{y}^2}\right] - \rho g - \sigma\bar{B}^2\bar{u}, \tag{1}$$

$$\rho\left[\bar{u}\frac{\partial\bar{v}}{\partial\bar{x}} + \bar{v}\frac{\partial\bar{v}}{\partial\bar{y}}\right] = -\frac{\partial\bar{p}}{\partial\bar{y}} + \mu\left[\frac{\partial^2\bar{v}}{\partial\bar{x}^2} + \frac{\partial^2\bar{v}}{\partial\bar{y}^2}\right]. \tag{2}$$

The continuity equation:

$$\frac{\partial\bar{u}}{\partial\bar{x}} + \frac{\partial\bar{v}}{\partial\bar{y}} = 0. \tag{3}$$

The energy equation:

$$\rho C_p\left[\bar{u}\frac{\partial\bar{T}}{\partial\bar{x}} + \bar{v}\frac{\partial\bar{T}}{\partial\bar{y}}\right]$$

$$= \kappa\left[\frac{\partial^2\bar{T}}{\partial\bar{x}^2} + \frac{\partial^2\bar{T}}{\partial\bar{y}^2}\right] + \frac{\rho D_M K_T}{C_S}\left[\frac{\partial^2\bar{C}}{\partial\bar{x}^2} + \frac{\partial^2\bar{C}}{\partial\bar{y}^2}\right] + Q - \frac{\partial\bar{q}_r}{\partial\bar{y}}. \tag{4}$$

The species continuity equation:

$$\bar{u}\,\frac{\partial \bar{C}}{\partial \bar{x}} + \bar{v}\,\frac{\partial \bar{C}}{\partial \bar{y}} = D_M\left[\frac{\partial^2 \bar{C}}{\partial \bar{x}^2} + \frac{\partial^2 \bar{C}}{\partial \bar{y}^2}\right] + \frac{D_M K_T}{T_m}\left[\frac{\partial^2 \bar{T}}{\partial \bar{x}^2} + \frac{\partial^2 \bar{T}}{\partial \bar{y}^2}\right]. \tag{5}$$

The radiation heat flux $\bar{q}_r$ as emphasized by Cogley et al. [21] for an optically thin fluid is given by

$$\frac{\partial \bar{q}_r}{\partial \bar{y}} = 4I(\bar{T} - \bar{T}_S), \tag{6}$$

where $I = \int_0^\infty (K_\lambda)_w \left(\frac{\partial e_{b\lambda}}{\partial \bar{T}}\right)_w d\lambda.$

In static condition, (1) takes the form

$$0 = -\frac{\partial \bar{p}_s}{\partial \bar{x}} - \rho_s g. \tag{7}$$

Now, (1)-(7) yield

$$\rho\left[\bar{u}\,\frac{\partial \bar{u}}{\partial \bar{x}} + \bar{v}\,\frac{\partial \bar{u}}{\partial \bar{y}}\right] = -\frac{\partial}{\partial \bar{x}}(\bar{p} - \bar{p}_s) + g(\rho_s - \rho) + \mu\left[\frac{\partial^2 \bar{u}}{\partial \bar{x}^2} + \frac{\partial^2 \bar{u}}{\partial \bar{y}^2}\right] - \sigma B^2 \bar{u}. \tag{8}$$

The equation of state is

$$\rho = \rho_s[1 - \beta(\bar{T} - \bar{T}_s) - \bar{\beta}(\bar{C} - \bar{C}_s)]. \tag{9}$$

Equations (8) and (9) together give

$$\rho\left[\bar{u}\,\frac{\partial \bar{u}}{\partial \bar{x}} + \bar{v}\,\frac{\partial \bar{u}}{\partial \bar{y}}\right] = -\frac{\partial}{\partial \bar{x}}(\bar{\rho} - \bar{\rho}_s) + \rho g[\beta(\bar{T} - \bar{T}_s) + \bar{\beta}(\bar{C} - \bar{C}_s)]$$

$$+ \mu\left[\frac{\partial^2 \bar{u}}{\partial \bar{x}^2} + \frac{\partial^2 \bar{u}}{\partial \bar{y}^2}\right] - \sigma B^2 \bar{u}. \tag{10}$$

The boundary conditions are

$$\bar{y} = \bar{\varepsilon} \cos k\bar{x} : \bar{u} = \bar{v} = 0;\ \bar{T} = \bar{T}_w;\ \bar{C} = \bar{C}_w, \tag{11}$$

$$\bar{y} = d : \bar{u} = \bar{v} = 0;\ \bar{T} = \bar{T}_1;\ \bar{C} = \bar{C}_1. \tag{12}$$

We define the following non-dimensional quantities:

$$x = \frac{\bar{x}}{d},\ y = \frac{\bar{y}}{d},\ u = \frac{\bar{u}d}{\upsilon},\ v = \frac{\bar{v}d}{\upsilon},\ p = \frac{\bar{p}d^2}{\rho\upsilon^2},$$

$$p_s = \frac{\bar{p}_s d^2}{\rho\upsilon^2},\ \lambda = kd,\ \varepsilon = \frac{\bar{\varepsilon}}{d},\ p_r = \frac{\mu C_p}{k},$$

$$G_r = \frac{d^3 g\beta(\bar{T}_w - \bar{T}_s)}{\upsilon^2},\ G_m = \frac{d^3 g\bar{\beta}(\bar{C}_w - \bar{C}_s)}{\upsilon^2},$$

$$n = \frac{\bar{C}_1 - \bar{C}_s}{\bar{C}_w - \bar{C}_s},\ m = \frac{\bar{T}_1 - \bar{T}_s}{\bar{T}_w - \bar{T}_s},$$

$$S_r = \frac{D_M K_T(\bar{T}_w - \bar{T}_s)}{\upsilon T_m(\bar{C}_w - \bar{C}_s)},\ D_u = \frac{D_M K_T(\bar{C}_w - \bar{C}_s)}{\upsilon C_s C_p(\bar{T}_w - \bar{T}_s)},$$

$$S_c = \frac{\upsilon}{D_M},\ M = \frac{\sigma B^2 d^2}{\rho\upsilon},$$

$$T = \frac{\bar{T} - \bar{T}_s}{\bar{T}_w - \bar{T}_s},\ C = \frac{\bar{C} - \bar{C}_s}{\bar{C}_w - \bar{C}_s},\ \alpha = \frac{Qd^2}{k(\bar{T}_w - \bar{T}_s)},\ N = \frac{4Id^2}{\rho\upsilon C_p}.$$

All physical variables and parameters are defined in the Nomenclature.

The governing equations in non-dimensional form are as under

$$u\frac{\partial u}{\partial x} + v\frac{\partial u}{\partial y} = -\frac{\partial}{\partial x}(p - p_s) + \frac{\partial^2 u}{\partial x^2} + \frac{\partial^2 u}{\partial y^2} + G_r T + G_m C - Mu, \tag{13}$$

$$u\frac{\partial v}{\partial x} + v\frac{\partial v}{\partial y} = -\frac{\partial p}{\partial y} + \frac{\partial^2 v}{\partial x^2} + \frac{\partial^2 v}{\partial y^2}, \tag{14}$$

$$\frac{\partial^2 T}{\partial x^2} + \frac{\partial^2 T}{\partial y^2} + P_r D_u\left(\frac{\partial^2 C}{\partial x^2} + \frac{\partial^2 C}{\partial y^2}\right) = P_r\left(u\frac{\partial T}{\partial x} + v\frac{\partial T}{\partial y}\right) - \alpha + P_r NT, \tag{15}$$

$$\frac{1}{S_c}\left(\frac{\partial^2 C}{\partial x^2} + \frac{\partial^2 C}{\partial y^2}\right) + S_r\left(\frac{\partial^2 T}{\partial x^2} + \frac{\partial^2 T}{\partial y^2}\right) = u\frac{\partial C}{\partial x} + v\frac{\partial C}{\partial y}, \tag{16}$$

$$\frac{\partial u}{\partial x} + \frac{\partial v}{\partial y} = 0 \tag{17}$$

with the boundary conditions:

$$u = 0,\ v = 0,\ T = 1,\ C = 1 \text{ on } y = \varepsilon \cos \lambda x, \tag{18}$$

$$u = 0,\ v = 0,\ T = m,\ C = n \text{ on } y = 1. \tag{19}$$

Method of Solutions

In order to solve equations (13) to (17), we assume u, v, p, T and C as follows:

$$u(x,\ y) = u_0(y) + \varepsilon u_1(x,\ y) + \cdots, \tag{20.1}$$

$$v(x,\ y) = \varepsilon v_1(x,\ y) + \cdots, \tag{20.2}$$

$$p(x,\ y) = p_0(x) + \varepsilon p_1(x,\ y) + \cdots, \tag{20.3}$$

$$T(x,\ y) = T_0(y) + \varepsilon T_1(x,\ y) + \cdots, \tag{20.4}$$

$$C(x,\ y) = C_0(y) + \varepsilon C_1(x,\ y) + \cdots. \tag{20.5}$$

By substituting the transformations (20.1) to (20.5) in (13) to (17), and by equating the coefficients of ε^0, ε^1 and neglecting the higher powers of ε and assuming $\frac{\partial}{\partial x}(p_0 - p_s) = 0$ (Ostrach [1]), we derive the following set of ordinary differential equations:

$$\frac{d^2 u_0}{dy^2} - M u_0 = -G_r T_0 - G_m C_0, \tag{21}$$

$$\frac{d^2 T_0}{dy^2} + P_r D_u \frac{d^2 C_0}{dy^2} = -\alpha + P_r N T_0, \tag{22}$$

$$\frac{d^2 C_0}{dy^2} + S_r S_c \frac{d^2 T_0}{dy^2} = 0, \tag{23}$$

$$u_0 \frac{\partial u_1}{\partial x} + v_1 \frac{du_0}{dy} = -\frac{\partial p_1}{\partial x} + \frac{\partial^2 u_1}{\partial x^2} + \frac{\partial^2 u_1}{\partial y^2} + G_r T_1 + G_m C_1 - M u_1, \tag{24}$$

$$u_0 \frac{\partial v_1}{\partial x} = -\frac{\partial p_1}{\partial y} + \frac{\partial^2 v_1}{\partial x^2} + \frac{\partial^2 v_1}{\partial y^2}, \tag{25}$$

$$\frac{\partial u_1}{\partial x} + \frac{\partial v_1}{\partial y} = 0, \tag{26}$$

$$\frac{\partial^2 T_1}{\partial x^2} + \frac{\partial^2 T_1}{\partial y^2} + P_r D_u \left(\frac{\partial^2 C_1}{\partial x^2} + \frac{\partial^2 C_1}{\partial y^2} \right) = P_r \left(u_0 \frac{\partial T_1}{\partial x} + v_1 \frac{dT_0}{dy} \right) + P_r N T_1, \tag{27}$$

$$\frac{1}{S_c} \left(\frac{\partial^2 C_1}{\partial x^2} + \frac{\partial^2 C_1}{\partial y^2} \right) + S_r \left(\frac{\partial^2 T_1}{\partial x^2} + \frac{\partial^2 T_1}{\partial y^2} \right) = u_0 \frac{\partial C_1}{\partial x} + v_1 \frac{dC_0}{dy} \tag{28}$$

subject to the boundary conditions:

$$u_0 = 0, \quad T_0 = 1, \quad C_0 = 1 \quad \text{at} \quad y = 0,$$

$$u_0 = 0, \quad T_0 = m, \quad C_0 = n \quad \text{at} \quad y = 1, \tag{29}$$

$$u_1 = -Re[u_0'(0) e^{i\lambda x}], \quad v_1 = 0, \quad T_1 = -Re[T_0'(0) e^{i\lambda x}],$$

$$C_1 = -Re[C_0'(0) e^{i\lambda x}] \quad \text{at} \quad y = 0,$$

$$u_1 = 0, \quad v_1 = 0, \quad T_1 = 0, \quad C_1 = 0 \quad \text{at} \quad y = 1. \tag{30}$$

The solutions of equations (21), (22) and (23) subject to the boundary conditions (29) are:

$$u_0(y) = A_{20} e^{\sqrt{M} y} + A_{19} e^{-\sqrt{M} y} + A_{15} e^{A_1 y} + A_{16} e^{A_2 y} + A_{18} y + A_{17}, \tag{31}$$

$$T_0(y) = A_4 e^{A_1 y} + A_3 e^{A_2 y} + A_5, \tag{32}$$

$$C_0(y) = A_8 e^{A_1 y} + A_9 e^{A_2 y} + A_7 y + A_{10}, \tag{33}$$

where

$$A_1 = \sqrt{\frac{P_r N}{1 - S_c S_r P_r D_u}}, \; A_2 = -A_1,$$

$$A_3 = \frac{1}{e^{A_2} - e^{A_1}}\left(m - \frac{\alpha}{P_r N}\right) - \frac{e^{A_1}}{e^{A_2} - e^{A_1}}\left(1 - \frac{\alpha}{P_r N}\right),$$

$$A_4 = 1 - \frac{\alpha}{P_r N} - A_3,\ A_5 = \frac{\alpha}{P_r N},$$

$$A_6 = n + S_c S_r (A_4 e^{A_1} + A_3 e^{A_2}),$$

$$A_{10} = 1 + S_c S_r (A_4 + A_3),\ A_7 = A_6 - A_{10},$$

$$A_8 = -S_c S_r A_4,\ A_9 = -S_c S_r A_3,$$

$$A_{11} = -(G_r A_4 + G_m A_8),\ A_{12} = -(G_r A_3 + G_m A_9),$$

$$A_{13} = -G_m A_7,\ A_{14} = -(G_r A_5 + G_m A_{10}),$$

$$A_{15} = \frac{A_{11}}{A_1^2 - M},\ A_{16} = \frac{A_{12}}{A_2^2 - M},$$

$$A_{17} = -A_{14}/M,\ A_{18} = -A_{13}/M,$$

$$A_{19} = -\frac{1}{e^{\sqrt{M}} - e^{-\sqrt{M}}}$$

$$\cdot [(A_{15} + A_{16} + A_{17})e^{\sqrt{M}} - A_{15}e^{A_1} - A_{16}e^{A_2} - A_{17} - A_{18}],$$

$$A_{20} = -A_{19} - A_{15} - A_{16} - A_{17}.$$

Now owing to get the solution of the first order equations, we introduce the stream function $\overline{\psi}_1$ defined by

$$u_1 = -\frac{\partial \overline{\psi}_1}{\partial y}, \quad v_1 = \frac{\partial \overline{\psi}_1}{\partial x}. \tag{34}$$

On elimination of p, equations (24), (25), (27) and (28) yield

$$u_0(\overline{\psi}_{1,\,xyy} + \overline{\psi}_{1,\,xxx}) - u_0''\overline{\psi}_{1,\,x}$$

$$= \overline{\psi}_{1,\,xxxx} + 2\overline{\psi}_{1,\,xxyy} + \overline{\psi}_{1,\,yyyy} - G_r T_{1,\,y} - G_m C_{1,\,y} - M\,\overline{\psi}_{1,\,yy}, \tag{35}$$

$$T_{1,xx} + T_{1,yy} + P_r D_u (C_{1,xx} + C_{1,yy}) = P_r (u_0 T_{1,x} + \overline{\psi}_{1,x} T_0') + P_r N T_1, \quad (36)$$

$$\frac{1}{S_c}(C_{1,xx} + C_{1,yy}) + S_r (T_{1,xx} + T_{1,yy}) = u_0 C_{1,x} + \overline{\psi}_{1,x} C_0'. \quad (37)$$

Considering the transformations $\overline{\psi}_1 = e^{i\lambda x}\psi(y)$, $T_1 = e^{i\lambda x}\theta(y)$, $C_1 = e^{i\lambda x}\phi(y)$, equations (35), (36) and (37) reduce to

$$\psi^{iv} - \psi''(i\lambda u_0 + 2\lambda^2 + M) + \psi(i\lambda u_0'' + i\lambda^3 u_0 + \lambda^4) = G_r \theta' + G_m \phi', \quad (38)$$

$$\theta'' - \theta'(\lambda^2 + P_r N + P_r u_0 i\lambda) + P_r D_u (-\lambda^2 \phi + \phi'') = P_r i\lambda \psi T_0', \quad (39)$$

$$\phi'' - \phi(\lambda^2 + S_c u_0 i\lambda) + S_c S_r (-\lambda^2 \theta + \theta'') = i\lambda S_c \psi C_0' \quad (40)$$

subject to the relevant boundary conditions:

$$\psi'(y) = u_0'(0), \quad \psi(y) = 0, \quad \theta(y) = -T_0'(0), \quad \phi(y) = -C_0'(0) \text{ at } y = 0, \quad (41)$$

$$\psi'(y) = 0, \quad \psi(y) = 0, \quad \theta(y) = 0, \quad \phi(y) = 0 \text{ at } y = 1. \quad (42)$$

We assume the series expansion for ψ, θ and ϕ as follows:

$$\psi = \psi_0(y) + \lambda\psi_1(y) + \lambda^2\psi_2(y) + \cdots, \quad (43)$$

$$\theta = \theta_0(y) + \lambda\theta_1(y) + \lambda^2\theta_2(y) + \cdots, \quad (44)$$

$$\phi = \phi_0(y) + \lambda\phi_1(y) + \lambda^2\phi_2(y) + \cdots. \quad (45)$$

Substituting (43), (44) and (45) in equations (38), (39), (40), (41) and (42) and by equating the coefficients of λ^0, λ^1 and λ^2, and neglecting the terms of order greater than or equal to $O(\lambda^3)$, the following ordinary differential equations are obtained:

$$\psi_0^{iv} - M\psi_0'' = G_r \theta_0' + G_m \phi_0', \quad (46)$$

$$\psi_1^{iv} - iu_0\psi_0'' - M\psi_1'' + iu_0''\psi_0 = G_r \theta_1' + G_m \phi_1', \quad (47)$$

$$\psi_2^{iv} - M\psi_2'' - iu_0\psi_1'' + iu_0''\psi_1 - 2\psi_0'' = G_r \theta_2' + G_m \phi_2', \quad (48)$$

$$\theta_0^{iv} - P_r N\theta_0 + P_r D_u \phi_0'' = 0, \tag{49}$$

$$\theta_1^{iv} - P_r i u_0 \theta_0 - P_r N\theta_1 + P_r D_u \phi_1'' = P_r i\psi_0 T_0', \tag{50}$$

$$\theta_2^{iv} - \theta_0 - P_r N\theta_2 - P_r u_0 i\theta_1 - P_r D_u \phi_0 + P_r D_u \phi_2'' = P_r i\psi_1 T_0', \tag{51}$$

$$\phi_0'' + S_c S_r \theta_0'' = 0, \tag{52}$$

$$\phi_1'' + S_c S_r \theta_1'' = iS_c u_0 \phi_0 + iS_c C_0' \psi_0, \tag{53}$$

$$\phi_2'' - \phi_0 + S_c S_r (\theta_0'' - \theta_0) = iS_c u_0 \phi_1 + iS_c C_0' \psi_1 \tag{54}$$

subject to the boundary conditions:

$$\psi_0'(y) = u_0'(0), \quad \psi_0(y) = 0, \quad \theta_0(y) = -T_0'(0), \quad \phi_0(y) = -C_0'(0) \text{ at } y = 0,$$

$$\psi_0'(y) = 0, \quad \psi_0(y) = 0, \quad \theta_0(y) = 0, \quad \phi_0(y) = 0 \text{ at } y = 1, \tag{55}$$

$$\psi_1'(y) = 0, \quad \psi_1(y) = 0, \quad \theta_1(y) = 0, \quad \phi_1(y) = 0 \text{ at } y = 0,$$

$$\psi_1'(y) = 0, \quad \psi_1(y) = 0, \quad \theta_1(y) = 0, \quad \phi_1(y) = 0 \text{ at } y = 1, \tag{56}$$

$$\psi_2'(y) = 0, \quad \psi_2(y) = 0, \quad \theta_2(y) = 0, \quad \phi_2(y) = 0 \text{ at } y = 0,$$

$$\psi_2'(y) = 0, \quad \psi_2(y) = 0, \quad \theta_2(y) = 0, \quad \phi_2(y) = 0 \text{ at } y = 1. \tag{57}$$

The solutions of equations (46) to (54) subject to the boundary conditions (55), (56) and (57) are obtained but not presented here for the sake of brevity.

Skin Friction

The viscous drag per unit area at any point in the fluid in terms of skin friction $\bar{\tau}_{xy}$ is given by

$$\bar{\tau}_{xy} = \mu\left(\frac{\partial \bar{u}}{\partial \bar{y}} + \frac{\partial \bar{v}}{\partial \bar{x}}\right).$$

The non-dimensional skin friction τ_{xy} at any point is specified by

$$\tau_{xy} = \frac{d^2 \bar{\tau}_{xy}}{\rho \upsilon^2} = u_0'(y) + \varepsilon e^{i\lambda x} u_1'(y) + i\varepsilon\lambda e^{i\lambda x} v_1'(y).$$

At the wavy wall $y = \varepsilon \cos \lambda x,$ the coefficient of skin friction is given by

$$\tau_w = [\tau_{xy}]_{y=\varepsilon \cos \lambda x} = \tau_0^0 + \varepsilon Re[e^{i\lambda x} u_0''(0) + e^{i\lambda x} u_1'(0)],$$

where $\tau_0^0 = u_0'(0).$

At the flat wall $y = 1,$ the coefficient of skin friction is determined by

$$\tau_1 = [\tau_{xy}]_{y=1} = \tau_1^0 + \varepsilon Re[e^{i\lambda x} u_1'(1)],$$

where $\tau_1^0 = u_0'(1).$

Heat Transfer Coefficient

The non-dimensional heat transfer coefficient in terms of Nusselt number Nu is given by

$$Nu = \frac{\partial T}{\partial y} = T_0'(y) + \varepsilon \frac{\partial T_1}{\partial y} = T_0'(y) + \varepsilon e^{i\lambda x} \theta'(y).$$

At the wavy wall $y = \varepsilon \cos \lambda x,$ it is as under

$$\begin{aligned}
Nu_w &= \left[\frac{\partial \theta}{\partial y}\right]_{y=\varepsilon \cos \lambda x} \\
&= T_0'(\varepsilon \cos \lambda x) + \varepsilon e^{i\lambda x} \theta'(\varepsilon \cos \lambda x) \\
&= T_0'(0) + \varepsilon \cos \lambda x T_0''(0) + \varepsilon e^{i\lambda x}[\theta'(0) + \varepsilon \cos \lambda x \theta''(0)] \\
&= T_0'(0) + \varepsilon \cos \lambda x T_0''(0) + \varepsilon e^{i\lambda x} \theta'(0) \quad (\text{neglecting } \varepsilon^2) \\
&= Nu_0^0 + \varepsilon Re[e^{i\lambda x} T_0''(0) + e^{i\lambda x} \theta'(0)], \text{ where } Nu_0^0 = T_0'(0).
\end{aligned}$$

At the flat wall $y = 1,$ the Nusselt number is represented by

$$\begin{aligned}
Nu_1 &= \left[\frac{\partial \theta}{\partial y}\right]_{y=1} = T_0'(1) + \varepsilon e^{i\lambda x} \theta'(1) \\
&= Nu_1^0 + \varepsilon Re[e^{i\lambda x} \theta'(1)], \text{ where } Nu_1^0 = T_0'(1).
\end{aligned}$$

Mass Transfer Coefficient

The non-dimensional mass transfer coefficient in terms of Sherwood number Sh is given by

$$Sh = \frac{\partial C}{\partial y} = C_0'(y) + \varepsilon \frac{\partial C_1}{\partial y} = C_0'(y) + \varepsilon e^{i\lambda x}\phi(y).$$

At the wavy wall $y = \varepsilon \cos \lambda x$, the Sherwood number is as follows:

$$Sh_w = \left[\frac{\partial C}{\partial y}\right]_{y=\varepsilon\cos\lambda x} = C_0'(\varepsilon \cos \lambda x) + \varepsilon e^{i\lambda x}\phi'(\varepsilon \cos \lambda x)$$

$$= C_0'(0) + \varepsilon \cos \lambda x C_0''(0) + \varepsilon e^{i\lambda x}\phi'(0) \quad (\text{neglecting } \varepsilon^2)$$

$$= Sh_0^0 + \varepsilon Re[e^{i\lambda x}C_0''(0) + e^{i\lambda x}\phi'(0)], \text{ where } Sh_0^0 = C_0'(0).$$

At the flat wall $y = 1$, the Sherwood number is defined by

$$Sh_1 = \left[\frac{\partial C}{\partial y}\right]_{y=1} = C_0'(1) + \varepsilon e^{i\lambda x}\phi'(1) = Sh_1^0 + \varepsilon Re[e^{i\lambda x}\phi'(1)],$$

where $Sh_1^0 = C_0'(1)$.

Results and Discussion

In order to get physical insight into the problem, we have carried out numerical calculations for non-dimensional velocity field, temperature field, species concentration field and skin frictions at the walls by assigning some specific values to the parameters entering into the problem and the effects of these values on the above fields are demonstrated graphically. In our investigation, the values of the parameter λ (frequency parameter) and ε (amplitude parameter) are kept fixed at .001 and .01, respectively, and the values of the other parameters are chosen arbitrarily.

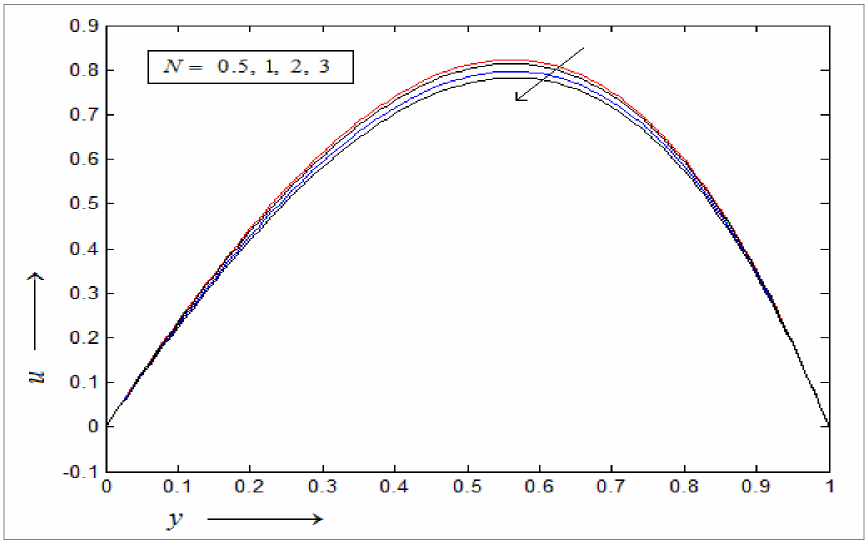

Figure 1. Velocity versus y under N for $P_r = .71$, $D_u = .2$, $M = .5$, $S_c = .6$, $S_r = 1$, $\alpha = 1$, $G_r = 2$, $G_m = 2$, $m = 5$, $n = 1$, $\lambda x = \pi/2$, $\lambda = .001$, $\varepsilon = .01$.

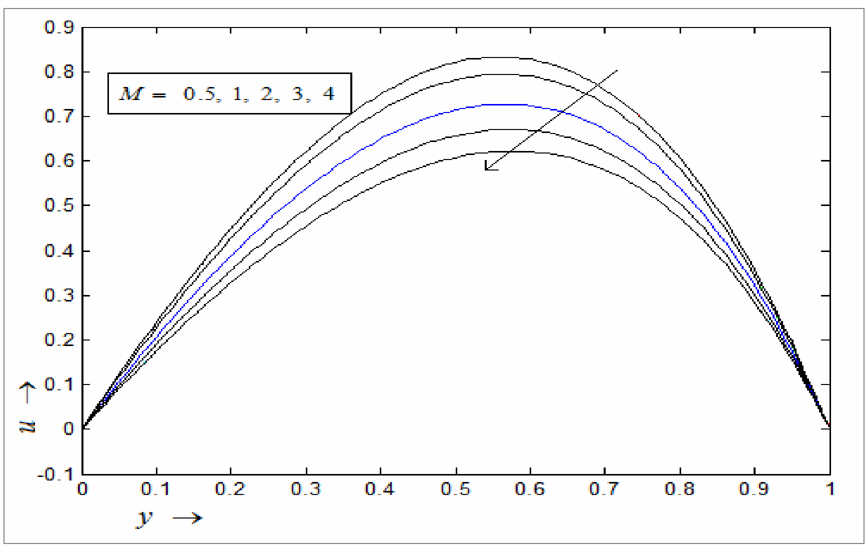

Figure 2. Velocity versus y under M for $P_r = .71$, $D_u = .2$, $S_c = .6$, $S_r = 1$, $\alpha = 1$, $G_r = 2$, $G_m = 2$, $m = 5$, $n = 1$, $N = 1$, $\lambda x = \pi/2$, $\lambda = .001$, $\varepsilon = .01$.

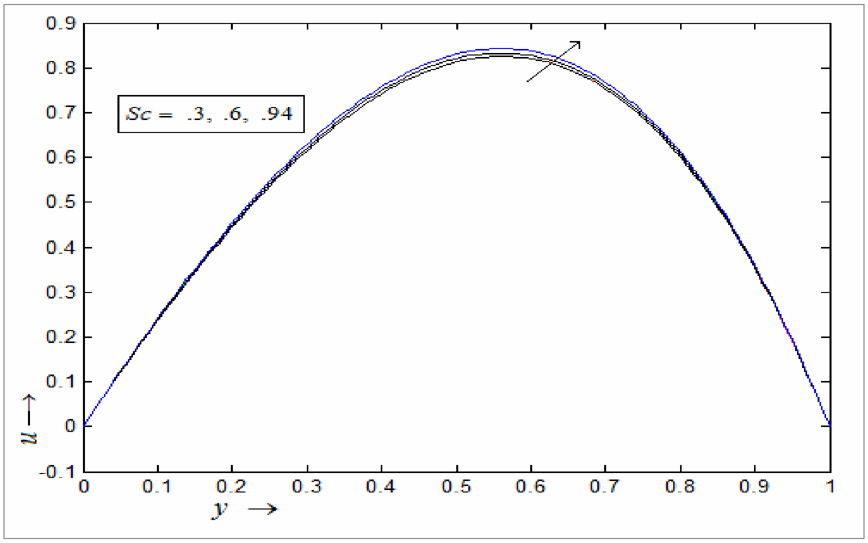

Figure 3. Velocity versus y under S_c for $P_r = .71$, $D_u = .2$, $M = .5$, $S_r = 1$, $\alpha = 1$, $G_r = 2$, $G_m = 2$, $m = 5$, $n = 1$, $N = 1$, $\lambda x = \pi/2$, $\lambda = .001$, $\varepsilon = .01$.

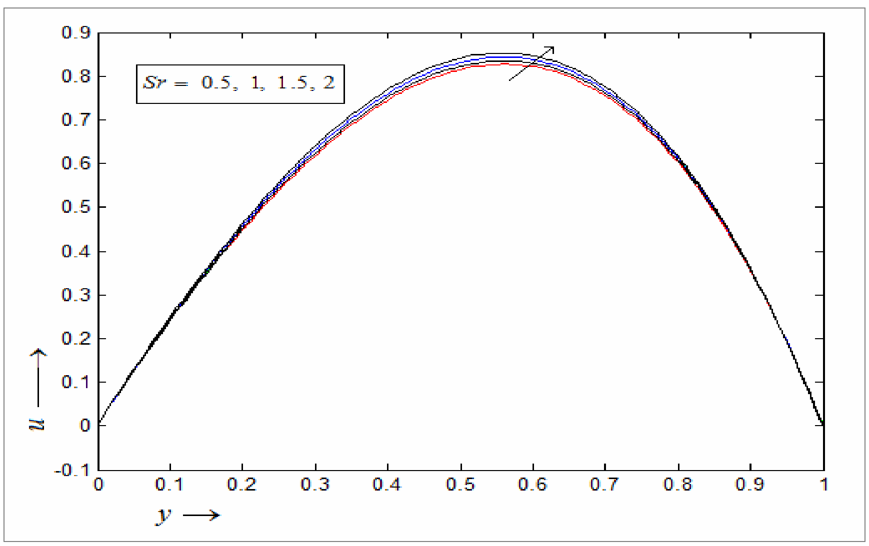

Figure 4. Velocity versus y under S_r for $P_r = .71$, $D_u = .2$, $M = .5$, $S_c = .6$, $\alpha = 1$, $G_r = 2$, $G_m = 2$, $m = 5$, $n = 1$, $N = 1$, $\lambda x = \pi/2$, $\lambda = .001$, $\varepsilon = .01$.

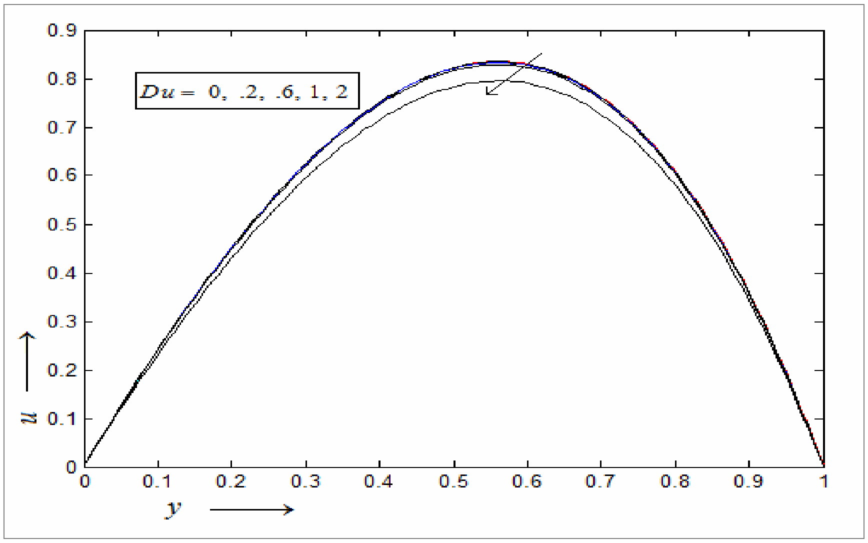

Figure 5. Velocity versus y under D_u for $P_r = .71$, $M = .5$, $S_c = .6$, $S_r = 1$, $\alpha = 1$, $G_r = 2$, $G_m = 2$, $m = 5$, $n = 1$, $N = 1$, $\lambda x = \pi/2$, $\lambda = .001$, $\varepsilon = .01$.

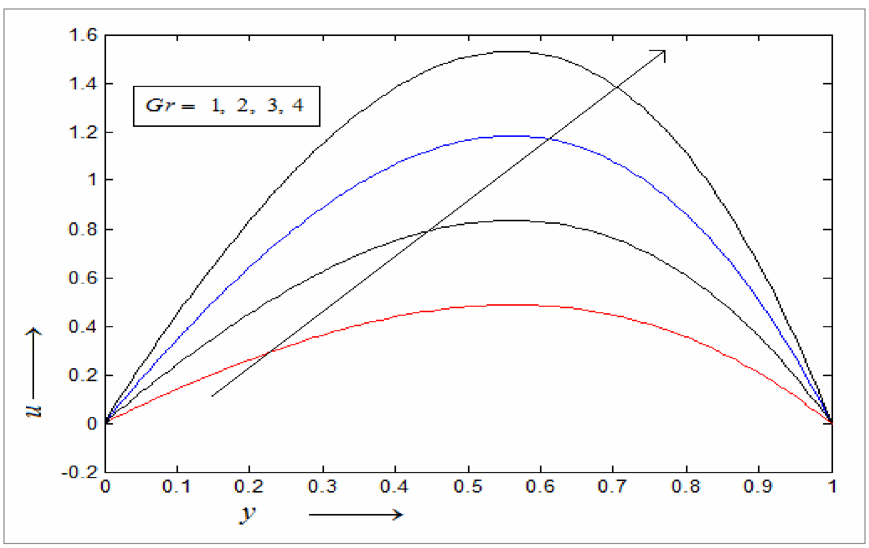

Figure 6. Velocity versus y under G_r for $P_r = .71$, $D_u = .2$, $M = .5$, $S_c = .6$, $S_r = 1$, $\alpha = 1$, $G_m = 2$, $m = 5$, $n = 1$, $N = 1$, $\lambda x = \pi/2$, $\lambda = .001$, $\varepsilon = .01$.

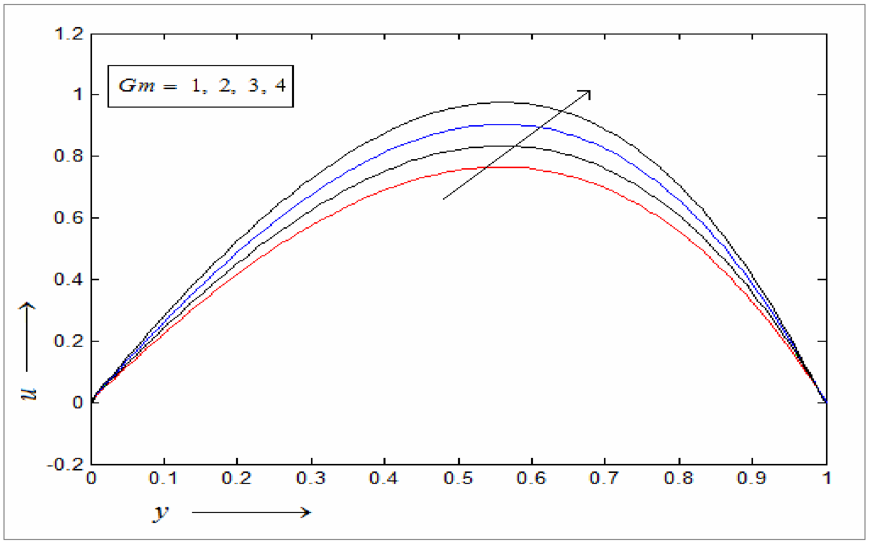

Figure 7. Velocity versus y under G_m for $P_r = .71,\ D_u = .2,\ M = .5,\ S_c = .6,$ $S_r = 1,\ \alpha = 1,\ G_r = 2,\ m = 5,\ n = 1,\ N = 1,\ \lambda x = \pi/2,\ \lambda = .001,\ \varepsilon = .01.$

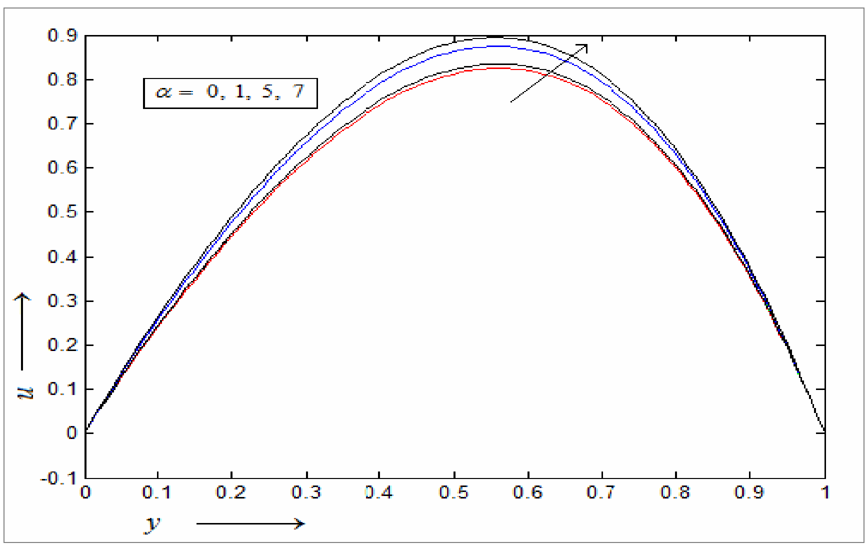

Figure 8. Velocity versus y under α for $P_r = .71,\ D_u = .2,\ M = .5,\ S_c = .6,$ $S_r = 1,\ G_r = 2,\ G_m = 2,\ m = 5,\ n = 1,\ N = 1,\ \lambda x = \pi/2,\ \lambda = .001,\ \varepsilon = .01.$

Figures 1-8 represent the variations of the velocity field *u* versus *y* under the effects of radiation parameter *N*, Hartmann number *M*, Schmidt number S_c, Soret number S_r, Dufour number D_u, Thermal Grashof number G_r, Solutal Grashof number G_m and heat generating source α. From these figures, we observe that the velocity field increases as S_c, S_r, G_r, G_m and α increase and decreases as *N*, *M* and D_u increase. It indicates the fact that the fluid motion is accelerated under the effect of thermal-diffusion, buoyancy forces (thermal and solutal) and heat generating source, whereas it is retarded due to the application of radiation, transverse magnetic field, diffusion-thermo, and mass diffusion. These figures further show that the velocity profiles exhibit a parabolic nature within the channel and the maximum velocity is attained at the middle of the channel. As such thermal radiation is an effective regulatory mechanism for controlling the flow pattern.

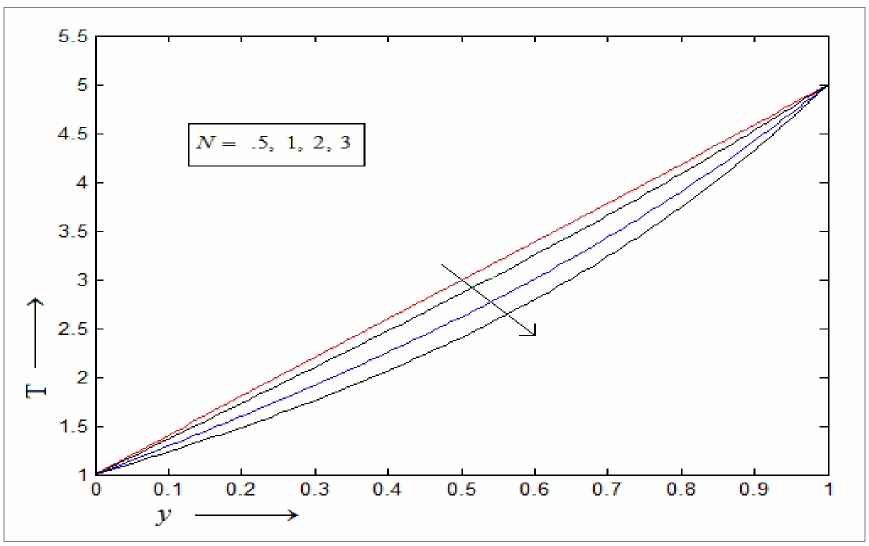

Figure 9. Temperature versus *y* under *N* for $P_r = .71$, $D_u = .2$, $M = .5$, $S_c = .6$, $S_r = 1$, $\alpha = 1$, $G_r = 2$, $G_m = 2$, $m = 5$, $n = 1$, $\lambda x = \pi/2$, $\lambda = .001$, $\varepsilon = .01$.

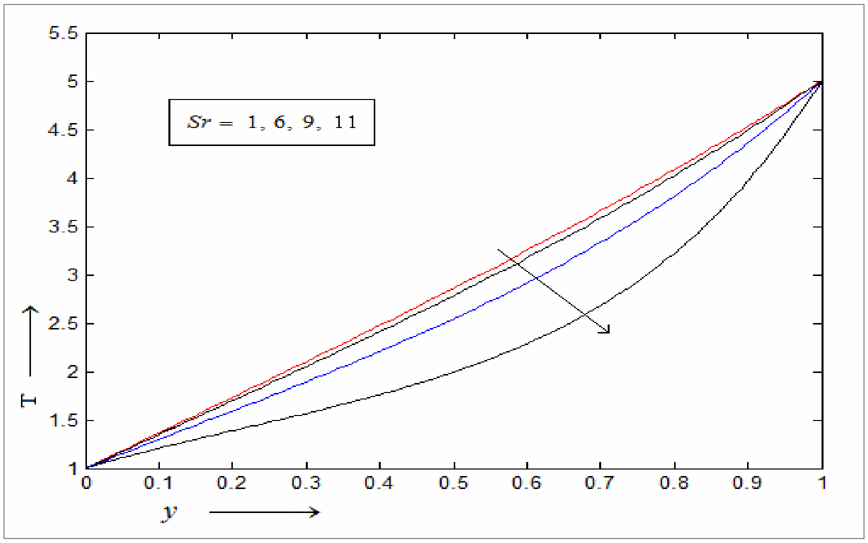

Figure 10. Temperature versus y under S_r for $P_r = .71$, $D_u = .2$, $M = .5$, $S_c = .6$, $\alpha = 1$, $G_r = 2$, $G_m = 2$, $m = 5$, $n = 1$, $N = 1$, $\lambda x = \pi/2$, $\lambda = .001$, $\varepsilon = .01$.

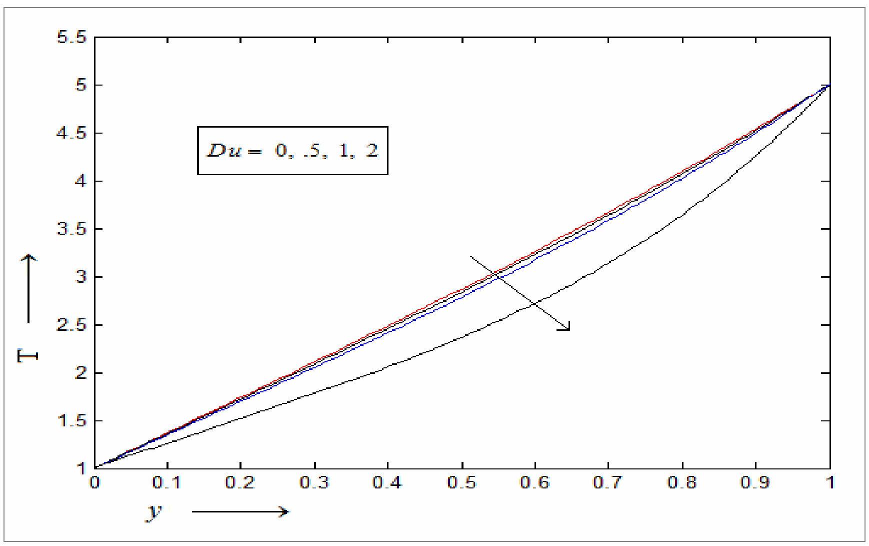

Figure 11. Temperature versus y under D_u for $P_r = .71$, $M = .5$, $S_c = .6$, $S_r = 1$, $\alpha = 1$, $Gr = 2$, $Gm = 2$, $m = 5$, $n = 1$, $N = 1$, $\lambda x = \pi/2$, $\lambda = .001$, $\varepsilon = .01$.

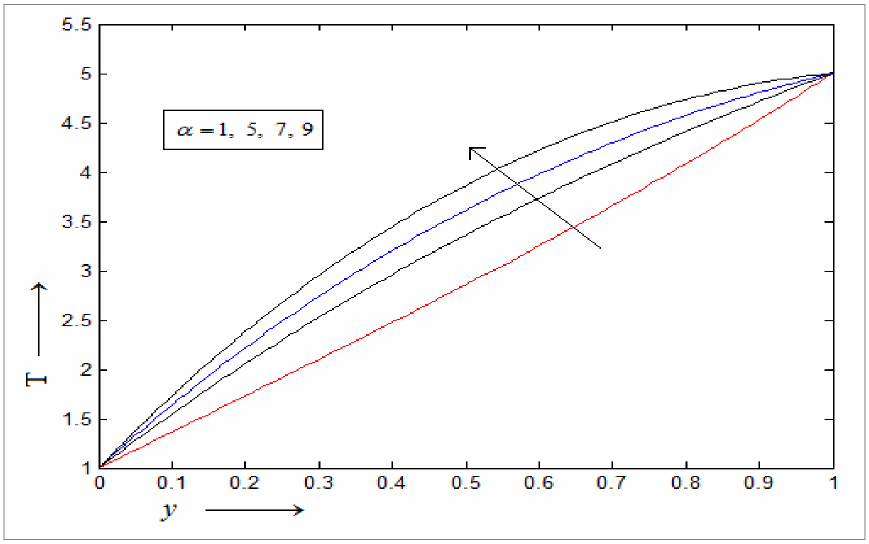

Figure 12. Temperature versus y under α for $P_r = .71$, $D_u = .2$, $M = .5$, $S_c = .6$, $S_r = 1$, $G_r = 2$, $G_m = 2$, $m = 5$, $n = 1$, $N = 1$, $\lambda x = \pi/2$, $\lambda = .001$, $\varepsilon = .01$.

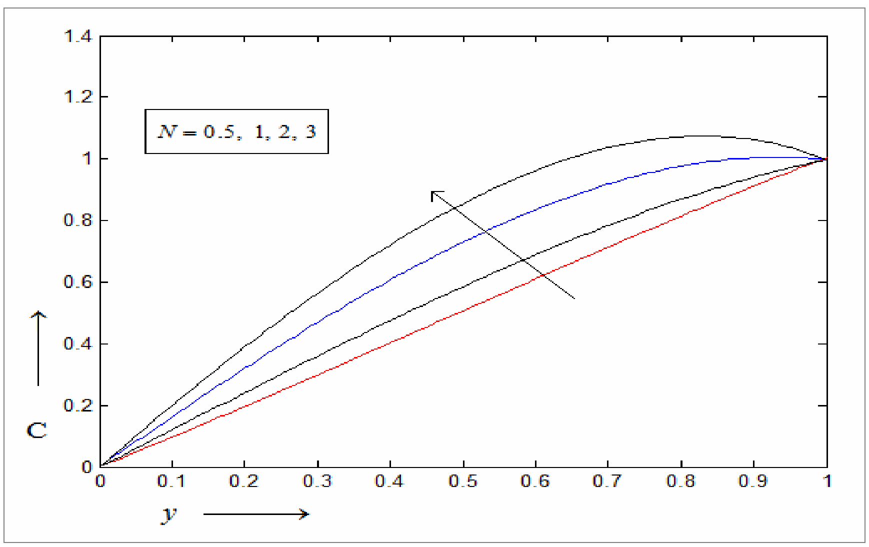

Figure 13. Concentration versus y under N for $P_r = .71$, $D_u = .2$, $M = .5$, $S_c = .6$, $S_r = 1$, $\alpha = 1$, $G_r = 2$, $G_m = 2$, $m = 5$, $n = 1$, $\lambda x = \pi/2$, $\lambda = .001$, $\varepsilon = .01$.

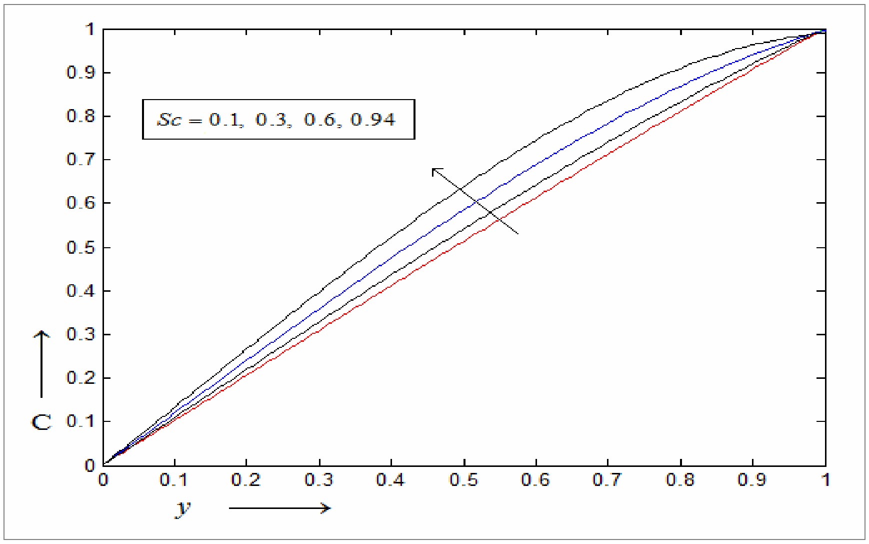

Figure 14. Concentration versus y under S_c for $P_r = .71$, $D_u = .2$, $M = .5$, $S_r = 1$, $\alpha = 1$, $G_r = 2$, $G_m = 2$, $m = 5$, $n = 1$, $N = 1$, $\lambda x = \pi/2$, $\lambda = .001$, $\varepsilon = .01$.

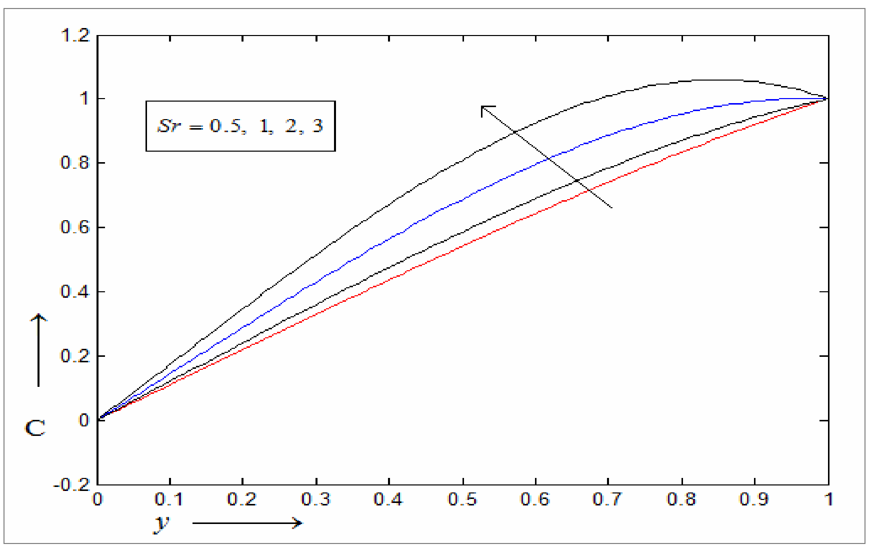

Figure 15. Concentration versus y under S_r for $P_r = .71$, $D_u = .2$, $M = .5$, $S_c = .6$, $\alpha = 1$, $G_r = 2$, $G_m = 2$, $m = 5$, $n = 1$, $N = 1$, $\lambda x = \pi/2$, $\lambda = .001$, $\varepsilon = .01$.

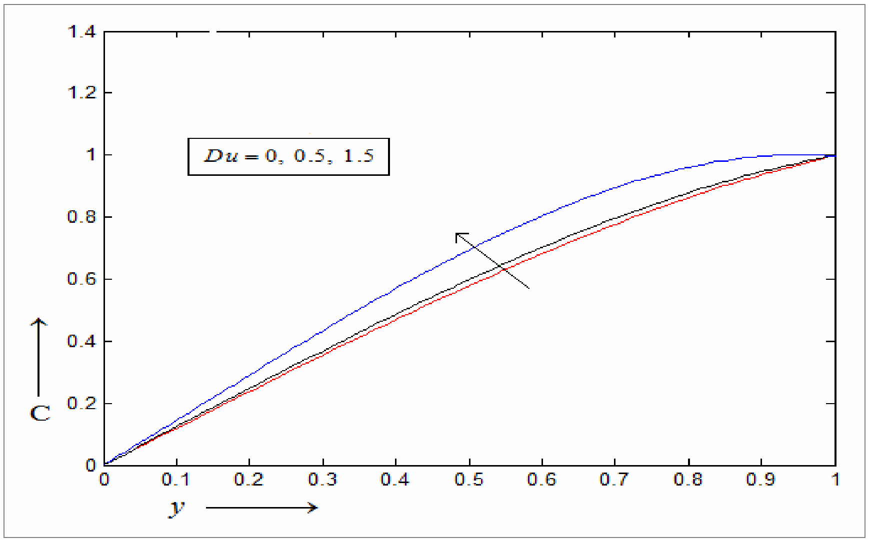

Figure 16. Concentration versus y under D_u for $P_r = .71,\ M = .5,\ S_c = .6,\ S_r = 1,\ \alpha = 1,\ G_r = 2,\ G_m = 2,\ m = 5,\ n = 1,\ N = 1,\ \lambda x = \pi/2,\ \lambda = .001,\ \varepsilon = .01.$

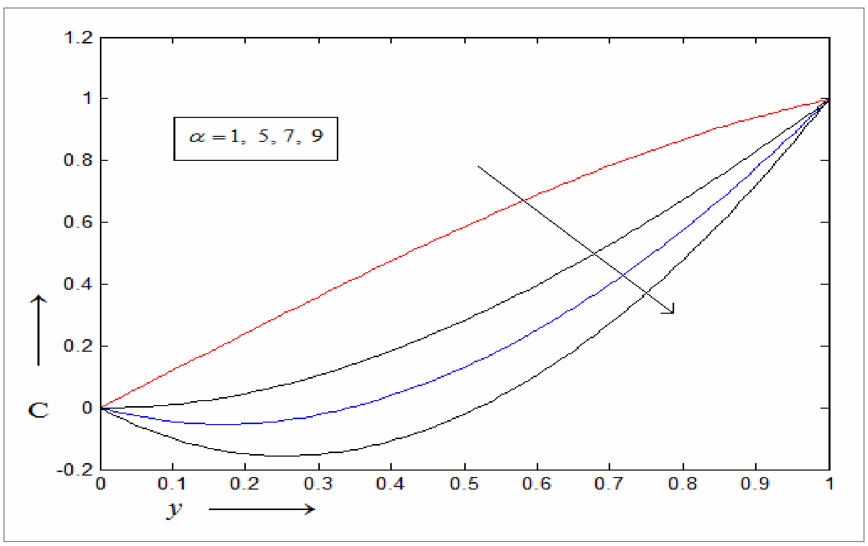

Figure 17. Concentration versus y under α for $P_r = .71,\ D_u = .2,\ M = .5,\ S_c = .6,\ S_r = 1,\ G_r = 2,\ G_m = 2,\ m = 5,\ n = 1,\ N = 1,\ \lambda x = \pi/2,\ \lambda = .001,\ \varepsilon = .01.$

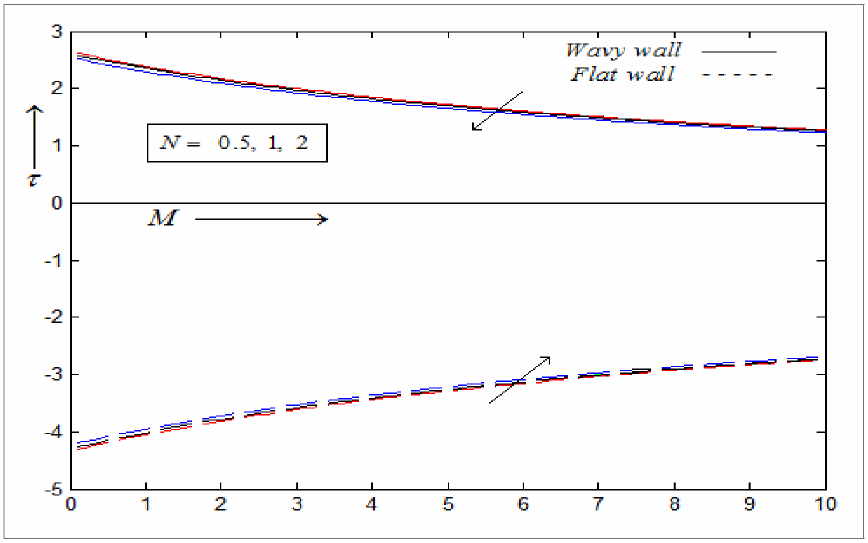

Figure 18. Skin friction τ versus M under N for $P_r = .71$, $D_u = .2$, $S_c = .6$, $S_r = 1$, $\alpha = 1$, $G_r = 2$, $G_m = 2$, $m = 5$, $n = 1$, $\lambda x = \pi/2$, $\lambda = .001$, $\varepsilon = .01$.

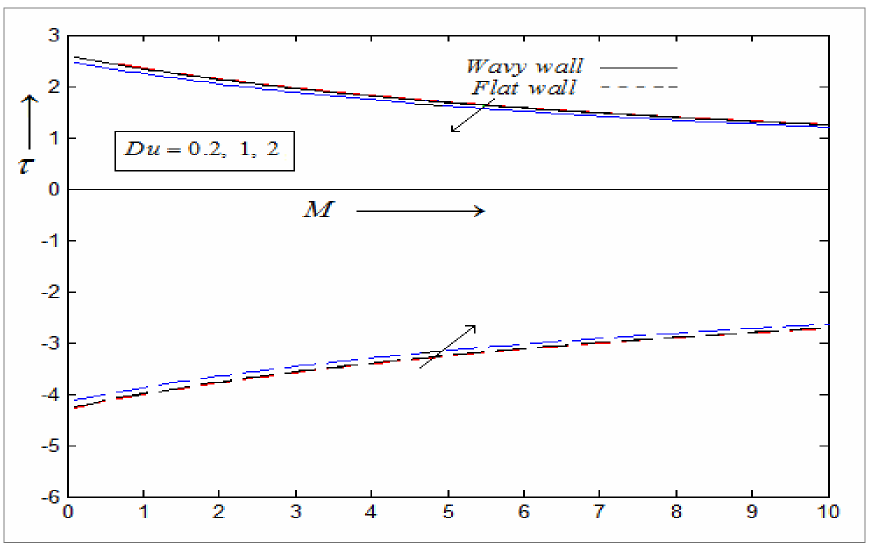

Figure 19. Skin friction τ versus M under D_u for $P_r = .71$, $S_c = .6$, $S_r = 1$, $\alpha = 1$, $G_r = 2$, $G_m = 2$, $m = 5$, $n = 1$, $N = 1$, $\lambda x = \pi/2$, $\lambda = .001$, $\varepsilon = .01$.

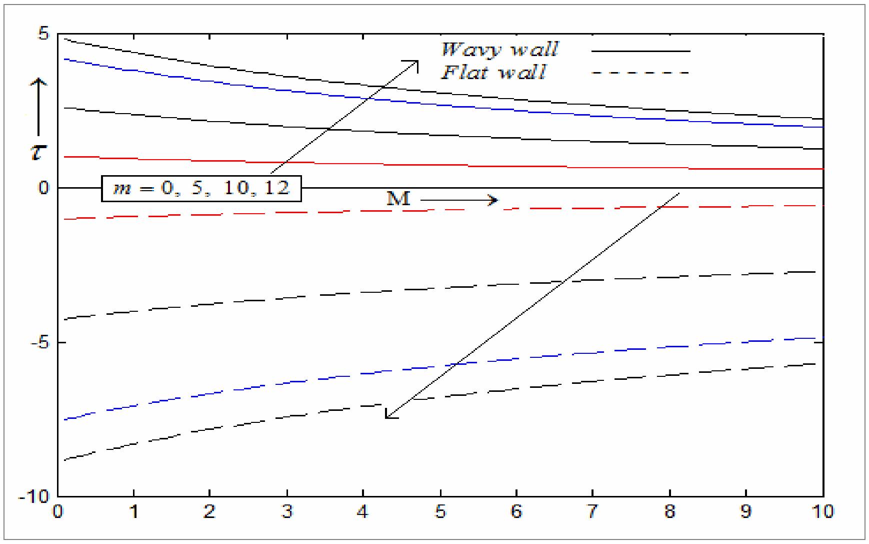

Figure 20. Skin friction τ versus M under m for $P_r = .71$, $D_u = .2$, $S_c = .6$, $S_r = 1$, $\alpha = 1$, $G_r = 2$, $G_m = 2$, $n = 1$, $N = 1$, $\lambda x = \pi/2$, $\lambda = .001$, $\varepsilon = .01$.

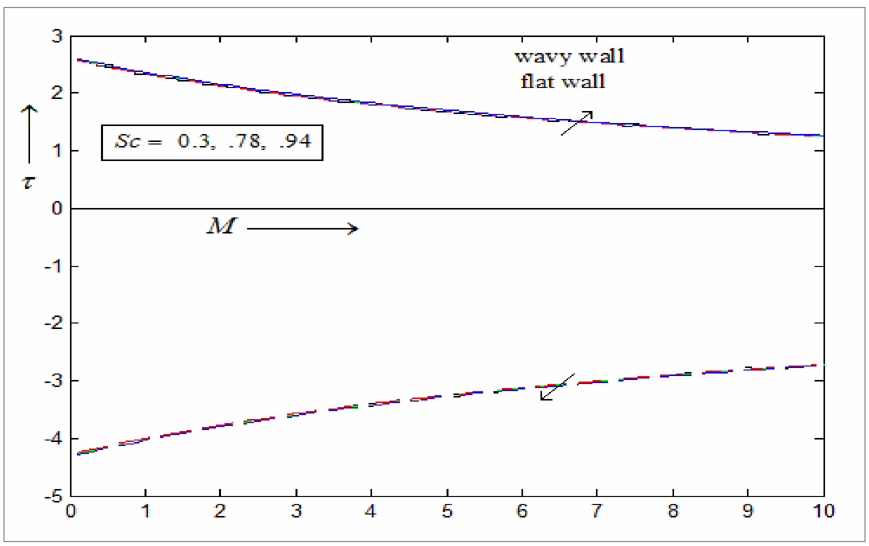

Figure 21. Skin friction τ versus M under S_c for $P_r = .71$, $D_u = .2$, $S_r = 1$, $\alpha = 1$, $G_r = 2$, $G_m = 2$, $m = 5$, $n = 1$, $N = 1$, $\lambda x = \pi/2$, $\lambda = .001$, $\varepsilon = .01$.

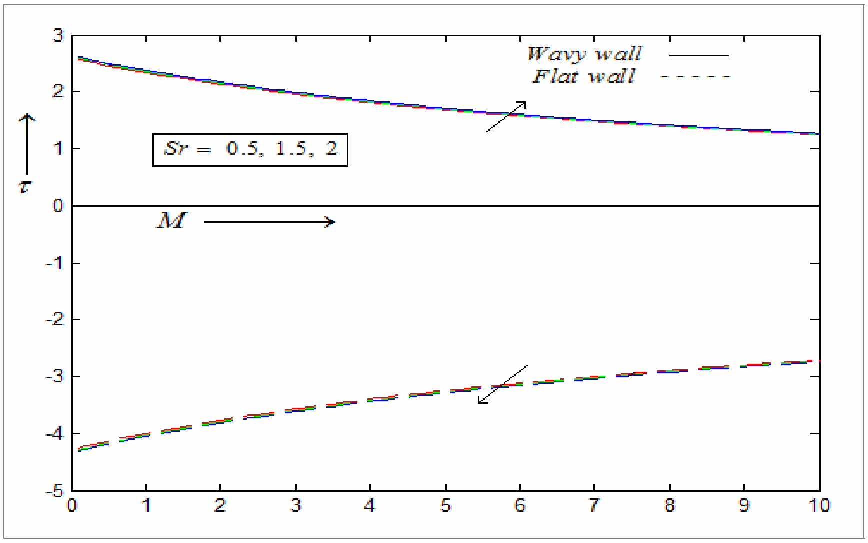

Figure 22. Skin friction τ versus M under S_r for $P_r = .71$, $D_u = .2$, $S_c = .6$, $\alpha = 1$, $G_r = 2$, $G_m = 2$, $m = 5$, $n = 1$, $N = 1$, $\lambda x = \pi/2$, $\lambda = .001$, $\varepsilon = .01$.

Figures 9-12 exhibit the behaviour of the temperature field against y under the influence of the parameters N, S_r, D_u and α. From the figures, it is clear that the fluid temperature increases as α increases and decreases as N, S_r and D_u increase. These figures show that the fluid temperature falls down due to the imposition of the radiation, thermal-diffusion and diffusion-thermo, but it rises up due to increasing value of heat generating source as expected.

The variation of species concentration C versus y under the influence of radiation parameter N, Schmidt number S_c, Soret number S_r, Dufour number D_u, and heat generating source α is presented in Figures 13, 14, 15, 16 and 17. These figures indicate that the concentration level of the fluid falls down due to the increasing values of α whereas the concentration level of the fluid raises up due to the increasing values of N, S_c, S_r and D_u. In other words, the thickness of the concentration boundary layer decreases under the effects of mass diffusion and heat generating source whereas the thickness of the concentration layer increases under the effects of thermal radiation, thermal-diffusion and diffusion-thermo. These observations are consistent with the physics of the problem.

The nature of skin friction τ at both the wavy wall and the flat wall is demonstrated in Figures 18, 19, 20, 21 and 22. It is observed from Figures 20 and 22 that the magnitudes of the viscous drag at both the walls rise up under the influence of increasing wall temperature ratio and Soret effect. But a reverse trend of behaviour of τ in case of radiation effect, Dufour effect and mass diffusion are marked in Figures 18, 19 and 21.

Comparison of Results

In order to highlight the accuracy of the numerical computation from the analytical solution in the present investigation, some of the results of the present work for some special case $(N = 50)$ have been compared with those of Ahmed et al. [16]. Comparing Figure 23 with Figure 24 (Figure 1 of Ahmed et al. [16]), we see that both figures uniquely indicate that the application of the transverse magnetic field causes the fluid flow to retard comprehensively. Hence there is a good agreement between the results obtained by Ahmed et al. [16] and the present authors.

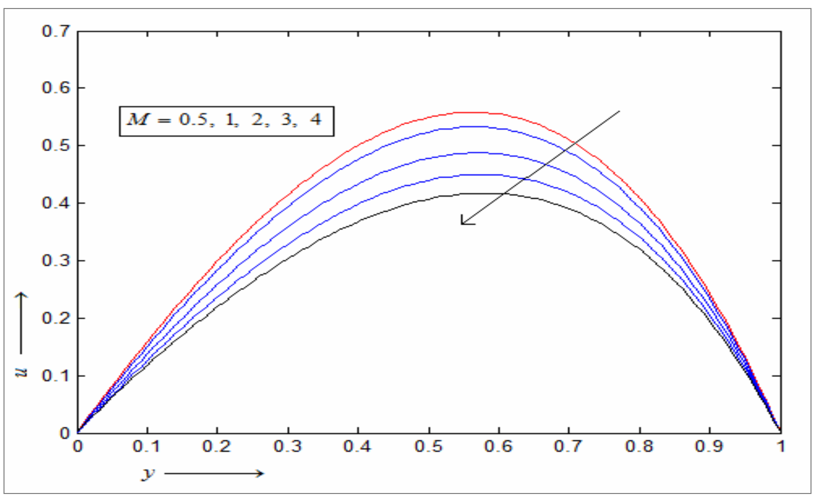

Figure 23. Velocity versus y under M for $P_r = .71$, $D_u = .2$, $S_c = .6$, $S_r = 1$, $\alpha = 1$, $G_r = 2$, $G_m = 2$, $m = 5$, $n = 1$, $N = 50$, $\lambda x = \pi/2$, $\lambda = .001$, $\varepsilon = .01$.

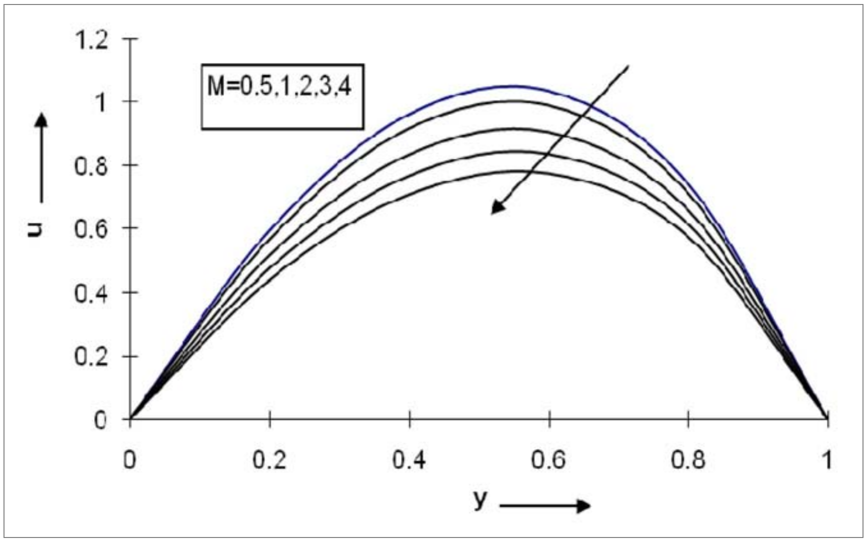

Figure 24. Velocity versus y under M for $P_r = .71,\ D_u = .2,\ S_c = .6,\ S_r = 1,$ $\alpha = 1,\ G_r = 2,\ G_m = 2,\ m = 5,\ n = 1,\ \lambda x = \pi/2,\ \lambda = .001,\ \varepsilon = .01.$

Conclusions

1. The fluid motion is retarded under the application of radiation, diffusion-thermo and the transverse magnetic field and accelerated due to thermal-diffusion effect.
2. An increase in radiation parameter, Soret number and Dufour number, tends the fluid temperature to fall.
3. The thickness of the concentration boundary layer increases under radiation, Soret and Dufour effects.
4. The thermal-radiation or diffusion-thermo effect leads the magnitude of the viscous drag at the wavy wall as well as the flat wall to decrease.
5. Finally, it is concluded that the radiation effect has a significant role in controlling the flow and transport characteristics.

References

[1] S. Ostrach, Laminar natural convective flow and heat transfer of fluid with and without heat sources in channel with constant wall temperature, N. A. C. A. Tech. Note. No. 2863, 1952.

[2] S. G. Lekoudis, A. H. Nayfeh and W. S. Saric, Compressible boundary layers over wavy walls, Phys. Fluids 19 (1976), 514-519.

[3] P. N. Shankar and U. N. Sinha, The Rayleigh problem for a wavy wall, J. Fluid Mech. 77 (1976), 243-256.

[4] M. Lessen and S. T. Gangwani, Effect of small amplitude wall waviness upon the stability of the boundary layers, Phys. Fluids 19 (1976), 510-513.

[5] K. Vajravelu and K. S. Sastri, Free convective heat transfer problem between a long vertical wavy wall and a parallel flat wall, J. Fluid Mech. 86 (1978), 365-383.

[6] C. N. B. Rao and K. S. Sastri, The response of skin-friction, wall heat transfer and pressure drop to wall waviness in the presence of buoyancy, Indian J. Math. Math. Sci. 5(3) (1982), 585-594.

[7] K. Vajravelu and K. S. Sastri, Natural convective heat transfer in vertical wavy channels. Int. J. Heat Mass Transfer 23 (1980), 408-411.

[8] C. N. B. Rao, Natural convective heat transfer of heat generating fluids in vertical channel with wavy walls, Rev. Roum. Phys. Tonu. 27(9) (1982), 783-799.

[9] U. N. Das and N. Ahmed, Free convective MHD flow and heat transfer in a viscous incompressible fluid confined between a long vertical wavy wall and a parallel flat wall, Indian J. Pure Appl. Math. 23(4) (1992), 295-304.

[10] E. R. G. Eckert and R. M. Drake, Analysis of Heat and Mass Transfer, McGraw-Hill, New York, 1972.

[11] Z. Dursunkaya and W. M. Worek, Diffusion-thermo and thermo-diffusion effects in transient and steady natural convection from vertical surface, Int. J. Heat Mass Transfer 35(8) (1992), 2060-2065.

[12] N. G. Kafoussias and E. M. Williams, Thermal-diffusion and diffusion-thermo effects on mixed free forced convective and mass transfer boundary layer flow with temperature dependent viscosity, Int. J. Eng. Sci. 33 (1995), 1369-1384.

[13] M. A. Sattar and M. M. Alam, Thermal-diffusion as well as transpiration effects on MHD free convective and mass transfer flow past an accelerated vertical porous plate, Indian J. Pure Appl. Math. 25(6) (1994), 679-688.

[14] M. S. Alam, M. Rahman, A. Maleque and M. Ferdows, Dufour and Soret effects of steady MHD combined free-forced convective and mass transfer flow past a semi vertical plate, Thammasat Int. J. Sci. Tech. 11(2) (2006), 1-12.

[15] M. C. Raju, S. V. K. Verma, P. V. Reddy and S. Saha, Soret effect due to natural convection between heated inclined plates with magnetic field, J. Mech. Eng., ME 39(2) (2008), 65-70.

[16] N. Ahmed, K. Sarma and H. Deka, Soret and Dufour effects on an MHD free convective flow through a channel bounded by a long wavy wall and a parallel flat wall, Turkish J. Phys. (2013), to appear.

[17] M. A. Hossain and H. S. Takhar, Radiation effects on mixed connection along a vertical plate with uniform surface temperature, Heat and Mass Transfer 31(4) (1996), 243-248.

[18] N. Ahmed and H. K. Sarmah, The radiation effect on a transient MHD flow with mass transfer past an impulsively fixed infinite vertical plate, Int. J. Appl. Math. Mech. 5(5) (2009), 87-98.

[19] V. Rajesh and S. V. K. Varma, Radiation effects on MHD flow through a porous medium with variable temperature or variable mass diffusion, Int. J. Appl. Math. Mech. 6(11) (2010), 39-57.

[20] D. Ch Kesavaiah, P. V. Satyanarayana and S. Venkataramana, Effects of the chemical reaction and radiation absorption on an unsteady MHD convective heat and mass transfer flow past a semi-infinite vertical permeable moving plate embedded in a porous medium with heat source and suction, Int. J. Appl. Math. Mech. 7(1) (2011), 52-69.

[21] A. C. Cogley, S. E. Gilles and W. G. Vincenti, Differential approximation for radiative transfer in a nongrey gas near equilibrium, AIAA J. 6(3) (1968), 551-553.